Desiree Wanders,[1] Kirsten P. Stone,[1] Laura A. Forney,[1] Cory C. Cortez,[1] Kelly N. Dille,[1] Jacob Simon,[1] Mark Xu,[1] Elisabeth C. Hotard,[1] Inna A. Nikonorova,[2] Ashley P. Pettit,[2] Tracy G. Anthony,[2] and Thomas W. Gettys[1]

Role of GCN2-Independent Signaling Through a Noncanonical PERK/NRF2 Pathway in the Physiological Responses to Dietary Methionine Restriction

Diabetes 2016;65:1499–1510 | DOI: 10.2337/db15-1324

Restricting availability of essential amino acids (EAAs) limits aminoacylation of tRNAs by their cognate EAAs and activates the nutrient-sensing kinase, general control nonderepressible 2 (GCN2). Activated GCN2 phosphorylates eukaryotic initiation factor 2 (eIF2), altering gene-specific translation and initiating a transcriptional program collectively described as the integrated stress response (ISR). Central GCN2 activation by EAA deprivation is also linked to an acute aversive feeding response. Dietary methionine restriction (MR) produces a well-documented series of physiological responses (increased energy intake and expenditure, decreased adiposity, and increased insulin sensitivity), but the role of GCN2 in mediating them is unknown. Using *Gcn2*$^{-/-}$ mice, we found that the absence of GCN2 had no effect on the ability of MR to reduce body weight or adiposity, increase energy intake and expenditure, increase hepatic transcription and release of fibroblast growth factor 21, or improve insulin sensitivity. Interestingly, hepatic eIF2 phosphorylation by MR was uncompromised in *Gcn2*$^{-/-}$ mice. Instead, protein kinase R–like endoplasmic reticulum (ER) kinase (PERK) was activated in both intact and *Gcn2*$^{-/-}$ mice. PERK activation corresponded with induction of the ISR and the nuclear respiratory factor 2 antioxidant program but not ER stress. These data uncover a novel glutathione-sensing mechanism that functions independently of GCN2 to link dietary MR to its metabolic phenotype.

Dietary methionine restriction (MR) increases life span and produces a profile of physiological responses that confer resistance to metabolic disease (1–6), but the anatomical organization and molecular identity of the sensing and translational mechanisms are unknown. General control nonderepressible 2 (GCN2) is a potential mediator because it is activated by limited essential amino acid (EAA) availability. Activated GCN2 phosphorylates the α-subunit of eukaryotic initiation factor 2 (eIF2), altering gene-specific translation and initiating a cytoprotective transcriptional program collectively described as the integrated stress response (ISR) (7,8). Activating transcription factor 4 (ATF4), a basic leucine zipper transcription factor with important roles in glucose homeostasis, lipid metabolism, and energy expenditure (EE), is among the gene products preferentially translated after eIF2 phosphorylation (9,10). During amino acid insufficiency, ATF4 coordinates induction of hepatic fibroblast growth factor 21 (FGF21) and other metabolic genes (11,12). However, the relative importance of these individual signaling components (e.g., GCN2, eIF2, ATF4) in mediating the complex physiological responses to EAA restriction is largely unknown.

Loss-of-function models have been used to assess the role of GCN2 in the transcriptional, physiological, and behavioral responses to dietary EAA deprivation. Soon after their introduction, activation of GCN2 within the anterior piriform cortex triggers an acute aversive feeding response that is absent in mice lacking *Gcn2* (13,14). Leucine deprivation (LD) also produces a chronic anorexigenic response that is not compromised in *Gcn2*$^{-/-}$ mice (15,16). However, downregulation of hepatic lipogenic genes by LD does require GCN2 (15). Together, these findings illustrate that responses to dietary LD are

[1]Laboratory of Nutrient Sensing and Adipocyte Signaling, Pennington Biomedical Research Center, Baton Rouge, LA
[2]Department of Nutritional Sciences, Rutgers University, New Brunswick, NJ
Corresponding author: Thomas W. Gettys, thomas.gettys@pbrc.edu.
Received 22 September 2015 and accepted 23 February 2016.
D.W. is currently affiliated with the Department of Nutrition, Georgia State University, Atlanta, GA.

mediated through a combination of GCN2-dependent and -independent mechanisms. A comparison of the responses to LD and MR reveals shared features but also distinct differences, particularly, their opposite effects on food intake and lipogenic gene expression in adipose tissue (17). It remains to be established whether these differences are EAA specific or simply reflect different degrees of restriction, irrespective of the EAA being restricted. In either case, the importance of GCN2 in mediating the biological responses to dietary MR is unknown.

In response to different cellular stresses, three other eIF2 kinases participate in activation of the ISR (18–21). Several reports identify auxiliary or cooperative action between GCN2 and protein kinase R–like endoplasmic reticulum (ER) kinase (PERK) in phosphorylating eIF2 and translational control (22–24). However, the transcriptional profiles activated by each kinase are distinct (20). PERK, IRE-1, and ATF6 are all activated by accumulation of unfolded proteins in the ER, and each induces a different component of the unfolded protein response (UPR). The UPR is a multipart stress response that includes the ISR, and unresolved ER stress has been implicated in metabolic disorders associated with obesity and diabetes (25). While dietary LD does not activate PERK or the UPR, activation of the UPR does engage GCN2 in cell-cycle control and cellular fate during metabolic stress (22,24).

Our work comparing low-protein diets with dietary MR proposed the interesting possibility that hepatic detection of reduced EAAs from both diets produced integrated effects on energy balance and insulin sensitivity by inducing hepatic FGF21 (26,27). Although the acute effects of protein restriction on FGF21 and energy balance appear to be GCN2 dependent (26), we report here that GCN2 is not required for MR-dependent induction of hepatic FGF21, increased EE, or enhancement of insulin sensitivity. Instead, we propose that MR is activating the ISR and antioxidant response program in liver via a noncanonical PERK/nuclear respiratory factor 2 (NRF2) pathway that effectively senses and translates the metabolic responses to MR in the absence of GCN2.

RESEARCH DESIGN AND METHODS

Animals and Diets

Experiment 1

Four-week-old male wild-type (WT) (n = 16) and *Gcn2*$^{-/-}$ (n = 19) C57BL/6J mice were obtained from The Jackson Laboratory (Bar Harbor, ME), acclimated to a control (CON) diet for 1 week prior to phenotyping using a Comprehensive Laboratory Animal Monitoring System (Columbus Instruments, Columbus, OH). Mice were acclimated to the chambers overnight prior to measurements of O_2 consumption and CO_2 production at 16-min intervals for 18 days. All mice received the CON diet for 4 days prior to switching half the mice to the MR diet. Respiratory exchange ratio (RER) was calculated as the ratio of VCO_2 produced to VO_2 consumed. EE was calculated as follows: VO_2 * (3.815 + [1.232 * RER]) * 4.1868. Thereafter, food intake, body weights, and composition were measured weekly for 12 weeks. The mice were returned to the Oxymax for 4 days for measurement of EE, RERs, and activity. Thereafter, mice were killed and tissues were harvested.

The diets were formulated as extruded pellets. The energy content of both CON and MR diets was 15.96 kJ/g, with 18.9% of energy from fat (corn oil), 64.9% from carbohydrate, and 14.8% from a custom mixture of L-amino acids. The amino acid content of the diet on a weight basis was 14.1%. The CON diet contained 0.86% methionine, and the MR diet contained 0.17% methionine. Food and water were provided ad libitum, and lights were on 12 h/day from 7:00 A.M. to 7:00 P.M.

Experiment 2

The temporal development of transcriptional and biochemical responses to MR was examined in 128 WT mice acclimated to CON diet in a room with a reversed light cycle (7:00 P.M. lights on and 7:00 A.M. lights off) for 1 week beginning at 6 weeks of age. The mice were then trained to eat at lights out for a period of 10 days by removal of all food at lights on (7:00 P.M.). Food was restored at lights off (7:00 A.M.). After the initial 10 days of training, half of the mice were switched to the MR diet. In groups of 16, mice were killed after 3 h, 6 h, 9 h, 12 h, 2 days, 4 days, 6 days, and 8 days on their respective diets. A cohort of *Gcn2*$^{-/-}$ mice (n = 24) followed the same feeding paradigm, and mice were killed 6 h and 6 days after initiation of the diets.

Experiment 3

A third cohort of WT (n = 20) and *Gcn2*$^{-/-}$ (n = 20) mice was shipped to the Vanderbilt Phenotyping Center to undergo hyperinsulinemic-euglycemic clamps as previously described (27,28). Mice of each genotype were placed on the CON diet for 1 week before being randomized to the CON or MR diet for the following 8 weeks prior to surgery for catheter placement. After a 5-day recovery, clamps were performed in conscious mice after a 5-h fast. Insulin (2.5 mU/kg/min) was infused, along with a 50% dextrose solution at a variable rate to maintain euglycemia. Whole-body glucose turnover was assessed with a 5-μCi bolus of [^{3}H]glucose tracer 1.5 h before insulin treatment, followed by a 0.05 μCi/min infusion during the clamp. Insulin-stimulated glucose uptake in individual organs was determined using 2-deoxy-*d*-[1-^{14}C]glucose administered as a single bolus (13 μCi) 120 min after the start of clamp procedure. At t = 145 min, epididymal white adipose tissue (WAT), inguinal WAT (IWAT), brown adipose tissue (BAT), gastrocnemius, vastus lateralis, soleus, brain, and heart were harvested for analysis.

Experiment 4

WT (n = 12) and *Gcn2*$^{-/-}$ (n = 12) mice were acclimated to CON diet for 2 weeks. Then, half of each genotype was switched to a custom diet devoid of methionine (0% methionine). Mice were killed after 6 days on their respective diets and tissues were collected.

Experiment 5

WT mice (n = 24) were acclimated to the CON diet for 1 week beginning at 6 weeks of age. Then, eight mice were switched to the MR diet, eight mice were switched to an MR diet containing 0.2% cysteine, and the remaining mice stayed on the CON diet. After 8 weeks on the diets, EE was measured and all mice were killed. The BIOOXYTECH GSH/GSSG-412 Assay kit (Oxis Research, Portland, OR) was used to determine hepatic glutathione (GSH/GSSG) following the manufacturer's protocol.

Experiment 6

WT mice (n = 24) were acclimated to CON diet for 1 week beginning at 6 weeks of age. Then, eight mice were switched to the MR diet containing 0.12% methionine, eight mice were switched to the 0.12% MR diet containing 0.2% cysteine, and the remaining mice stayed on the CON diet. The mice were killed after 8 weeks on their respective diets.

Experiment 7

WT mice (n = 8) and *FGF21*$^{-/-}$ mice (n = 8) kindly provided by Dr. Steven Kliewer (University of Texas Southwestern) were acclimated to CON diet for 1 week beginning at 6 weeks of age. Then, four mice of each genotype were switched to the MR diet, while the remaining mice stayed on the CON diet. After 8 weeks of ad libitum consumption of their respective diets, EE was measured over 4 days in the respective groups as described above. Thereafter, mice were killed and IWAT was harvested.

Protein Extraction and Immunoblotting

For measurement of eIF2α and PERK phosphorylation, powdered liver tissue was homogenized in assay buffer (25 mmol/L HEPES, 2 mmol/L EDTA, 10 mmol/L dithiothreitol, 50 mmol/L sodium fluoride, 50 mmol/L β-glycerophosphate pentahydrate, 3 mmol/L benzamidine, 1 mmol/L sodium orthovanadate, 0.5% deoxycholate, 1% SDS, protease inhibitor cocktail [Sigma-Aldrich], and 1 mmol/L microcystin). Equivalent amounts of protein from each sample were separated by SDS-PAGE and transferred to polyvinylidene fluoride membranes. Blots were developed using enhanced chemiluminescence, and band densities were quantified using Alphaview SA Imaging Software (version 3.4.0). The phospho-eIF2α antibody was from Abcam (Cambridge, MA), total eIF2α antibody was from Santa Cruz (Dallas, TX), and the p-PERK and total PERK antibodies were from Cell Signaling Technology (Beverly, MA).

RNA Isolation and Quantitative Real-Time PCR

Total RNA was isolated using the RNeasy Mini Kit (QIAGEN, Valencia, CA). One microgram of total RNA was reverse transcribed to produce complementary DNA. Gene expression was measured by RT-PCR (Applied Biosystems, Foster City, CA), and expression of the corresponding mRNAs was normalized to cyclophilin.

Serum Analysis

Serum glucose was determined using a kit from Cayman Chemical (Ann Arbor, MI). Serum FGF21 and insulin were measured using ELISA kits from R&D Systems (Minneapolis, MN) and Millipore (Billerica, MA).

Data Analysis

Analysis of the data was conducted with Statistica (version 8.0; StatSoft, Inc.), using two-way ANOVA with genotype (WT and *Gcn2*$^{-/-}$) and diet (CON and MR) as main effects. Group means of variables of interest were compared using residual variance as the error term to test for effects of diet within genotype and genotype within diet using linear contrasts and the Bonferroni correction. Protection against type I errors was set at $\alpha = 0.05$.

RESULTS

Role of GCN2 in Effects of Dietary MR on Energy Balance

Experiment 1

Body weights of WT and *Gcn2*$^{-/-}$ mice on the CON diet did not differ at the beginning or end of the study, and

Table 1—Metabolic parameters in WT and *Gcn2*$^{-/-}$ mice fed CON or MR diet for 14 weeks

	WT		*Gcn2*$^{-/-}$	
	CON	MR	CON	MR
Initial body weight (g)	16.8 ± 0.60^a	17.0 ± 0.43^a	18.3 ± 0.65^a	18.9 ± 0.79^a
Final body weight (g)	32.6 ± 1.16^a	24.0 ± 0.66^b	29.1 ± 1.39^a	22.8 ± 0.67^b
Initial % adiposity	15.6 ± 0.60^a	14.8 ± 0.48^a	15.0 ± 0.72^a	15.1 ± 0.62^a
Final % adiposity	26.0 ± 1.3^a	13.9 ± 0.8^b	21.2 ± 1.6^a	14.5 ± 0.39^b
Food intake (kJ/day)*	51.7 ± 1.3^a	58.7 ± 2.2^b	45.1 ± 1.1^a	52.6 ± 1.3^b
Food intake (kJ/day/g)†	1.86 ± 0.02^a	2.58 ± 0.03^b	1.77 ± 0.02^a	2.43 ± 0.04^b
Insulin (ng/mL)	1.94 ± 0.32^a	0.85 ± 0.07^b	2.17 ± 0.28^a	1.14 ± 0.12^b
Glucose (mg/dL)	259 ± 7^a	221 ± 15^b	233 ± 11^a	213 ± 6^b
Serum triglycerides (mmol/L)	1.12 ± 0.05^a	0.81 ± 0.03^b	1.16 ± 0.06^a	0.94 ± 0.03^b

Serum measurements were taken after a 4-h fast after 14 weeks on diets. Data are presented as mean ± SEM. *The average food intake less spillage was determined over a 24-h period each week in mice of each genotype on each diet, converted to kJ, and expressed as average kJ/day/mouse for the 14-week study. †The average energy intake per day expressed per unit of body weight for the 14-week study. Means annotated with different letters within genotype differ at $P < 0.05$.

dietary MR reduced weight to the same extent in both genotypes (Table 1). Initial adiposity was comparable between genotypes, but *Gcn2*$^{-/-}$ mice on the CON diet added less fat than WT mice during the study (Table 1). MR decreased adiposity to 14% of body weight in both genotypes despite producing comparable increases in food intake (Table 1). Interestingly, CON-fed *Gcn2*$^{-/-}$ mice consumed 13% less food than CON-fed WT mice. However, on a body weight–adjusted basis, energy intake did not differ between genotypes, and MR increased energy intake by 39% in WT mice and 37% in *Gcn2*$^{-/-}$ mice (Table 1). These findings illustrate that MR increased the energy costs of maintenance and growth similarly in both genotypes.

Temporal Changes in EE After Initiation of Dietary MR

Experiment 1

GCN2 plays an essential role in the acute, conditioned aversive response to EAA deprivation (13,29,30) but not the longer-term effects of LD on food intake (15,16). Therefore, we initially examined the acute responses to MR and found that EE was significantly increased 5 days after introduction of the MR diet in WT mice (Fig. 1*A*). The magnitude of the effect increased over the subsequent 5 days (Fig. 1*A*) and was also evident after 12 weeks on the respective diets. This early diet-induced increase in EE was delayed and muted in *Gcn2*$^{-/-}$ mice, not appearing until 9 days, and increasing by a smaller amount compared with

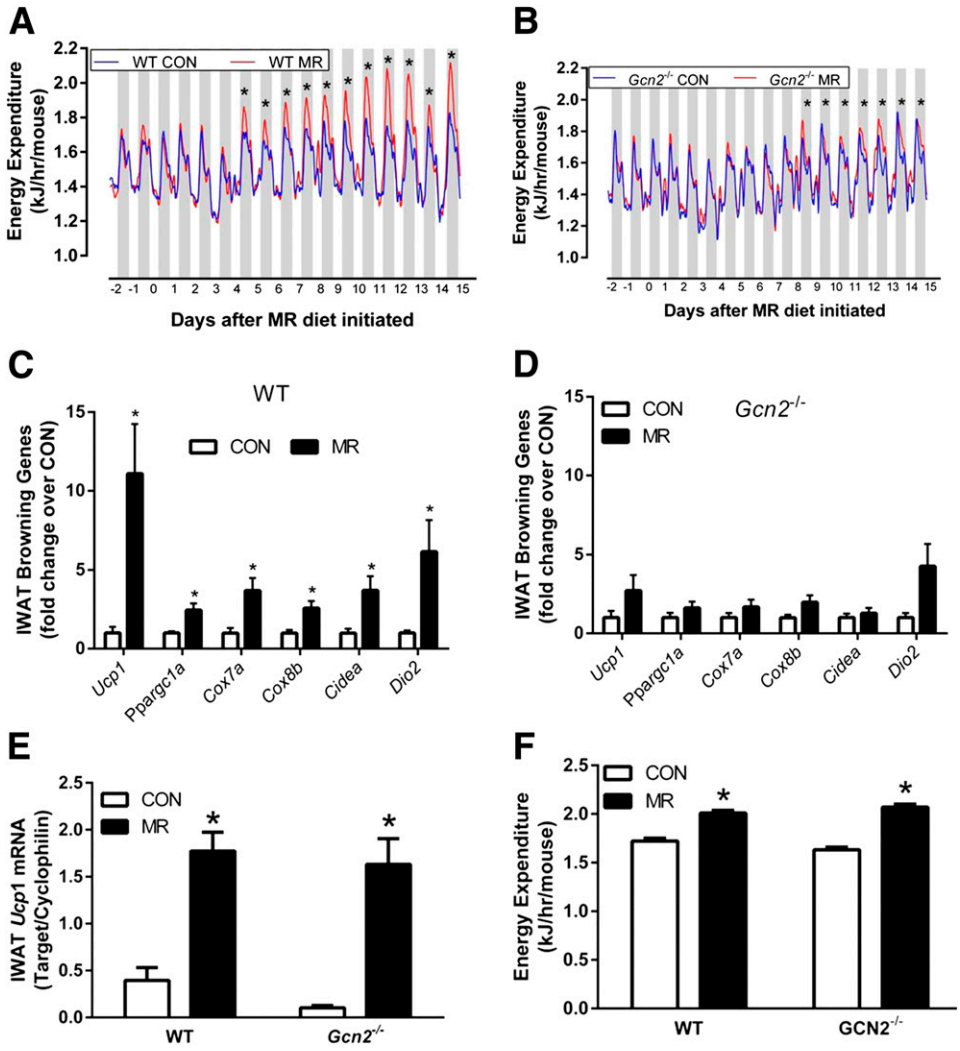

Figure 1—Time-dependent increase in EE and transcriptional markers of IWAT browning after introduction of dietary MR. EE was measured by indirect calorimetry in WT (*A*) and *Gcn2*$^{-/-}$ (*B*) mice. Mice were placed in the Oxymax on CON and were randomized to remain on CON or switched to MR while in the Oxymax. The effect of diet on 24-h EE was compared for each day within genotype over the next 14 days. *Differ from mice on the CON diet at $P < 0.05$. mRNA expression of markers of WAT browning was measured in IWAT of WT (*C*) and *Gcn2*$^{-/-}$ (*D*) mice after 6 days of dietary MR. *Ucp1* mRNA expression in IWAT (*E*) of WT and *Gcn2*$^{-/-}$ mice after 14 weeks of dietary MR. Fold changes in expression of each gene were calculated relative to the CON group within genotype for *C* and *D*. Data are presented as mean ± SEM. *Differ from corresponding CON within genotype at $P < 0.05$. Mice were returned to the Oxymax after 12 weeks on diets to undergo indirect calorimetry (*F*). Data are presented as mean ± SEM. *Differ from mice on the CON diet at $P < 0.05$. hr, hour.

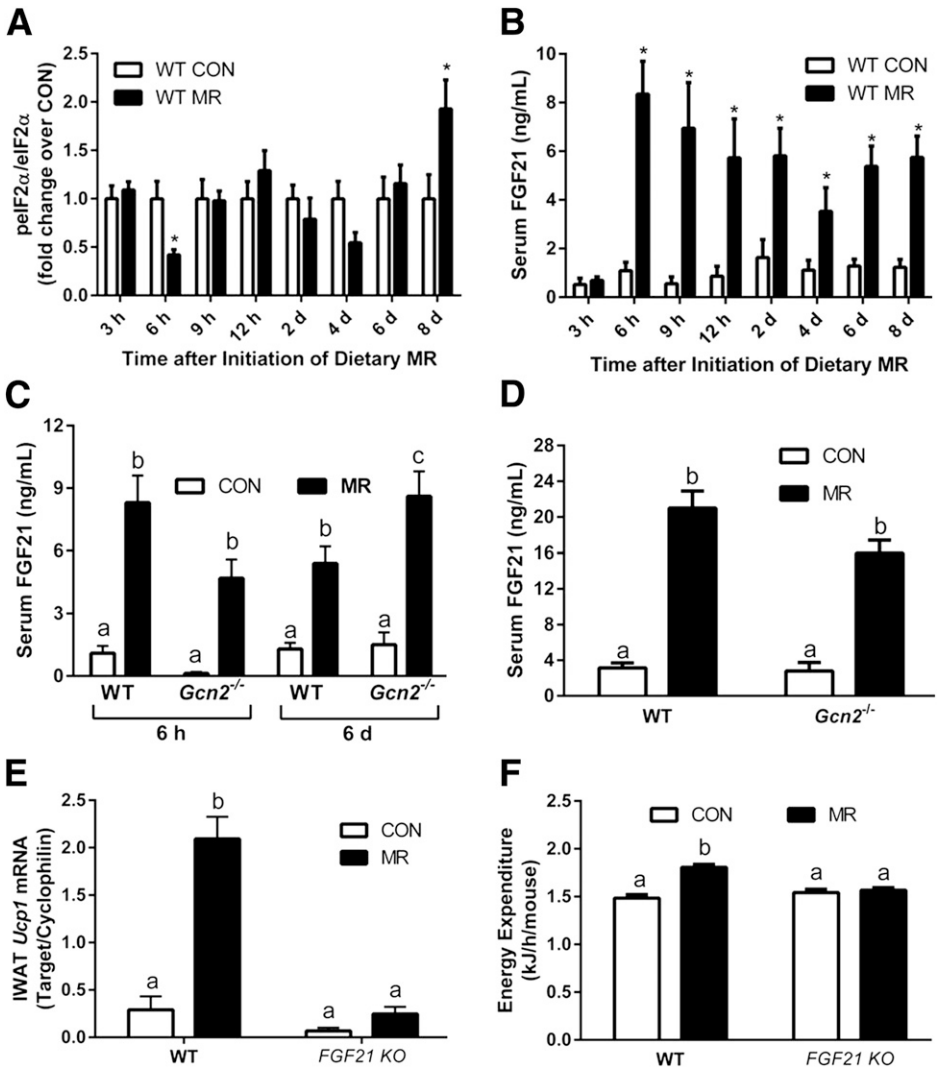

Figure 2—Effect of dietary MR on hepatic eIF2α phosphorylation (peIF2α) and FGF21, and role of FGF21 in effects of MR on UCP1 mRNA and total EE. eIF2α phosphorylation was measured by Western blot in livers of WT mice after 3, 6, 9, and 12 h and 2, 4, 6, and 8 days (d) of dietary MR. Band densities quantified and expressed as fold change in the MR group compared with CON (*A*). Corresponding measures of serum FGF21 in WT mice after 3, 6, 9, and 12 h and 2, 4, 6, and 8 days of dietary MR (*B*). Data for *A* and *B* are presented as mean ± SEM (n = 8). *Differ from corresponding CON at that time point. Serum FGF21 concentrations were measured 6 h and 6 days (*C*) or 14 weeks (*D*) after MR initiation in WT and *GCN2*$^{-/-}$ mice. Data are presented as mean ± SEM (n = 8), and means annotated with different letters differ within and across genotype at each time point at $P < 0.05$. IWAT UCP1 mRNA (*E*) and total EE (*F*) were measured in WT and *FGF21*$^{-/-}$ mice after 8 weeks of dietary MR. Data are presented as mean ± SEM (n = 4), and means annotated with different letters differ within and across genotype at $P < 0.05$. hr, hours; KO, knockout.

WT mice between 9 and 15 days (Fig. 1*A* and *B*). For example, the average MR-induced increase in EE after 2 weeks in the WT group was 12%, while the increase in *Gcn2*$^{-/-}$ mice was only 7% (Fig. 1*A* and *B*).

Time Course of Browning of WAT by MR

Experiments 1 and 2

Browning of WAT contributes to increased EE in rodents (31), and chronic MR (11 weeks) induces significant browning of WAT in mice (32). To explore the relationship between the acute increase in EE and the browning of WAT during MR, we measured thermogenic markers in IWAT after short- and long-term dietary MR. The MR diet increased markers of browning and thermogenesis (*Ucp1*, *Ppargc1a*, *Cox7a*, *Cox8b*, *Cidea*, and *Dio2*) within 6 days in WT mice (Fig. 1*C*) but not *Gcn2*$^{-/-}$ mice (Fig. 1*D*). However, after 14 weeks, MR increased mRNA expression of *Ucp1* in WAT to the same extent in WT and *Gcn2*$^{-/-}$ mice (Fig. 1*E*). These data show that the delayed increase in EE in *Gcn2*$^{-/-}$ mice after initiation of MR (Fig. 1*B*) is temporally related to a delayed induction of thermogenic genes in IWAT, whereas after chronic consumption of the diet, the increase in browning of WAT was comparable. In addition, measurement of EE after 12 weeks showed that the MR-induced increase in EE was comparable in WT and *Gcn2*$^{-/-}$ mice (Fig. 1*F*). Overall, the effects of MR on

energy balance were not compromised in *Gcn2*$^{-/-}$ mice (Table 1 and Fig. 1*F*).

Time Course of Hepatic eIF2 Phosphorylation and Induction of FGF21 After Initiation of Dietary MR

Experiments 1, 2, and 7

For examination of the relationship between eIF2 phosphorylation and FGF21 induction, WT mice were studied at different times after introduction of MR. A diet-induced increase in hepatic eIF2 phosphorylation was not detected before 8 days (Fig. 2*A*). In contrast, within 6 h of initiation of MR and at all subsequent time points, hepatic *Fgf21* mRNA (data not shown) and serum FGF21 (Fig. 2*B*) were significantly increased. Notwithstanding previous in vitro and in vivo findings linking eIF2 signaling to FGF21 expression (11,33), we find that eIF2 phosphorylation is not required for the acute MR-induced increase in hepatic FGF21.

To examine potential causes for the delayed increase in EE in *Gcn2*$^{-/-}$ mice after initiation of MR, we measured diet-induced induction of serum FGF21, a hormone that increases sympathetic nerve activity and EE (34–36). Dietary MR produced a 7.7-fold, 4.2-fold, and 6.8-fold increase in serum FGF21 after 6 h, 6 days, and 14 weeks, respectively, in WT mice, and at all three time points the MR diet produced comparable increases in serum FGF21 in *Gcn2*$^{-/-}$ mice (Fig. 2*C* and *D*). The fold increase in FGF21 in *Gcn2*$^{-/-}$ mice after 6 h was somewhat larger than the increase in WT mice, but by 6 days, both the net and fold increases were larger in *Gcn2*$^{-/-}$ mice (Fig. 2*C*). After 14 weeks, both basal and MR-induced levels of FGF21 were comparable between genotypes (Fig. 2*D*).

To examine the role of FGF21 in the MR-induced increase in adipocyte browning and increased EE, we measured MR-dependent induction of IWAT *Ucp1* mRNA and total EE in WT and *Fgf21*$^{-/-}$ mice. MR produced a four- to fivefold increase in *Ucp1* mRNA in WT mice but produced no detectable increase in *Ucp1* mRNA in IWAT from *Fgf21*$^{-/-}$ mice (Fig. 2*E*). Total EE was comparable in WT and *Fgf21*$^{-/-}$ mice on the CON diet, while MR increased EE by 22% in the WT mice (Fig. 2*F*). In contrast, MR failed to increase EE in the *Fgf21*$^{-/-}$ mice (Fig. 2*F*), illustrating that the MR-dependent increase in FGF21 is functionally linked to the diet-induced increase in IWAT *Ucp1* mRNA and total EE.

GCN2 Is Not Required for MR-Induced Increase in Insulin Sensitivity

Experiment 3

Dietary MR for 8–10 weeks produces a two- to threefold increase in overall insulin sensitivity (27,32). Short-term LD also increases insulin sensitivity (37), ostensibly through a mechanism requiring GCN2 (38). To test whether GCN2 was also required for MR to increase

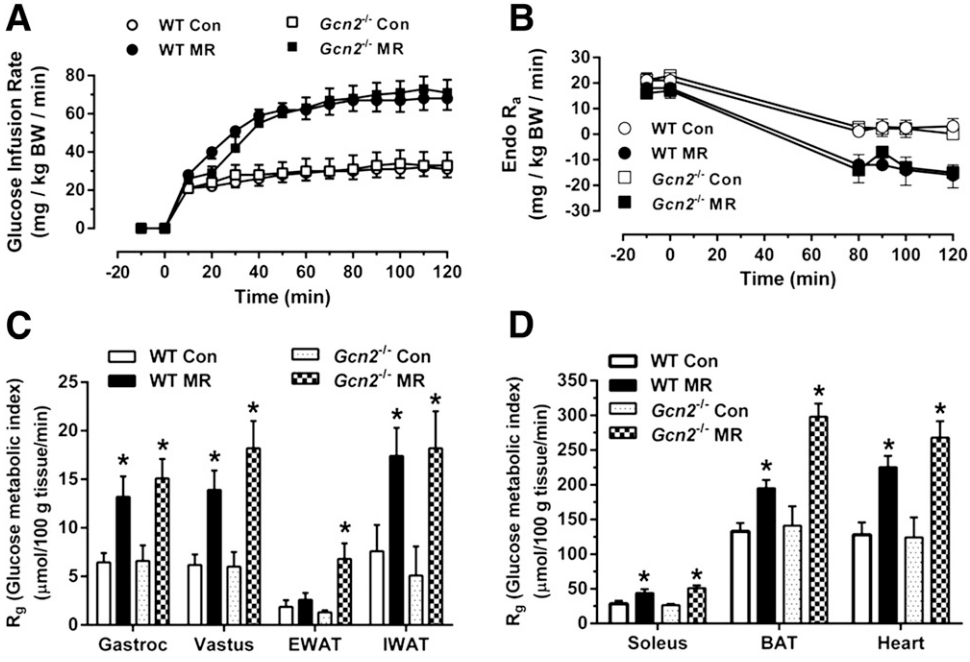

Figure 3—Hyperinsulinemic-euglycemic clamps in WT and *GCN2*$^{-/-}$ mice after 9 weeks of dietary MR to test for effects on overall insulin sensitivity and insulin-dependent 2-deoxyglucose uptake among tissues. The clamp procedures were conducted as described in RESEARCH DESIGN AND METHODS. *A*: The GIR required to maintain euglycemia during the insulin clamps. *B*: Effectiveness of insulin to suppress hepatic glucose production (% suppression of endo R_a) during the clamp procedure. *C* and *D*: R_g for each tissue. R_g provides a measure of insulin-dependent glucose uptake in each tissue. Plasma insulin levels during the clamp were as follows: WT CON, 1.4 ± 0.1 ng/mL; WT MR, 1.2 ± 0.1 ng/mL; *Gcn2*$^{-/-}$ CON, 1.4 ± 0.1 ng/mL; and *Gcn2*$^{-/-}$ MR, 1.0 ± 0.1 ng/mL. Means ± SEM are presented for each measurement and are based on n = 5–8 mice per genotype and diet. *Differ from CON within genotype at $P < 0.05$. BW, body wt; EWAT, epididymal WAT; Gastroc, gastrocnemius muscle; Vastus, vastus lateralis muscle.

insulin sensitivity, hyperinsulinemic-euglycemic clamps were used to compare the response between genotypes. The glucose infusion rates (GIRs) needed to establish euglycemia after initiating insulin infusion were achieved within 40 min in all groups, and steady-state glucose was maintained thereafter across the groups (Fig. 3*A*). The GIRs were indistinguishable in WT and *Gcn2*$^{-/-}$ mice on the CON diet (Fig. 3*A*) but were 2.2-fold higher in mice on the MR diet, regardless of genotype (Fig. 3*A*). Thus, the absence of GCN2 affected neither overall insulin sensitivity nor the responses of the mice to dietary MR. Liver 3-[^{3}H]glucose infusion was used to calculate basal endogenous glucose production (endo R_a) and compare insulin-dependent suppression of endo R_a during the clamp. Figure 3*B* shows that the efficacy of insulin to suppress hepatic glucose production was equivalently enhanced by MR in both genotypes. The glucose metabolic index (R_g) showed that MR produced significant two- to threefold increases in uptake of [^{14}C]2-deoxyglucose in gastrocnemius muscle, vastus lateralis muscle, soleus muscle, IWAT, BAT, and heart in both genotypes (Fig. 3*C* and *D*). Together, these data provide compelling evidence that GCN2 is not essential to the insulin-sensitizing effects of MR.

Alternative Signaling Paths to eIF2 From Dietary MR

Experiments 1 and 2

GCN2 is responsible for eIF2 phosphorylation in response to LD (39) and asparaginase treatment (40), as both responses are compromised in *Gcn2*$^{-/-}$ mice. In contrast, dietary MR increased phosphorylation of hepatic eIF2 by four- to fivefold in both genotypes (Fig. 4*A*), showing that

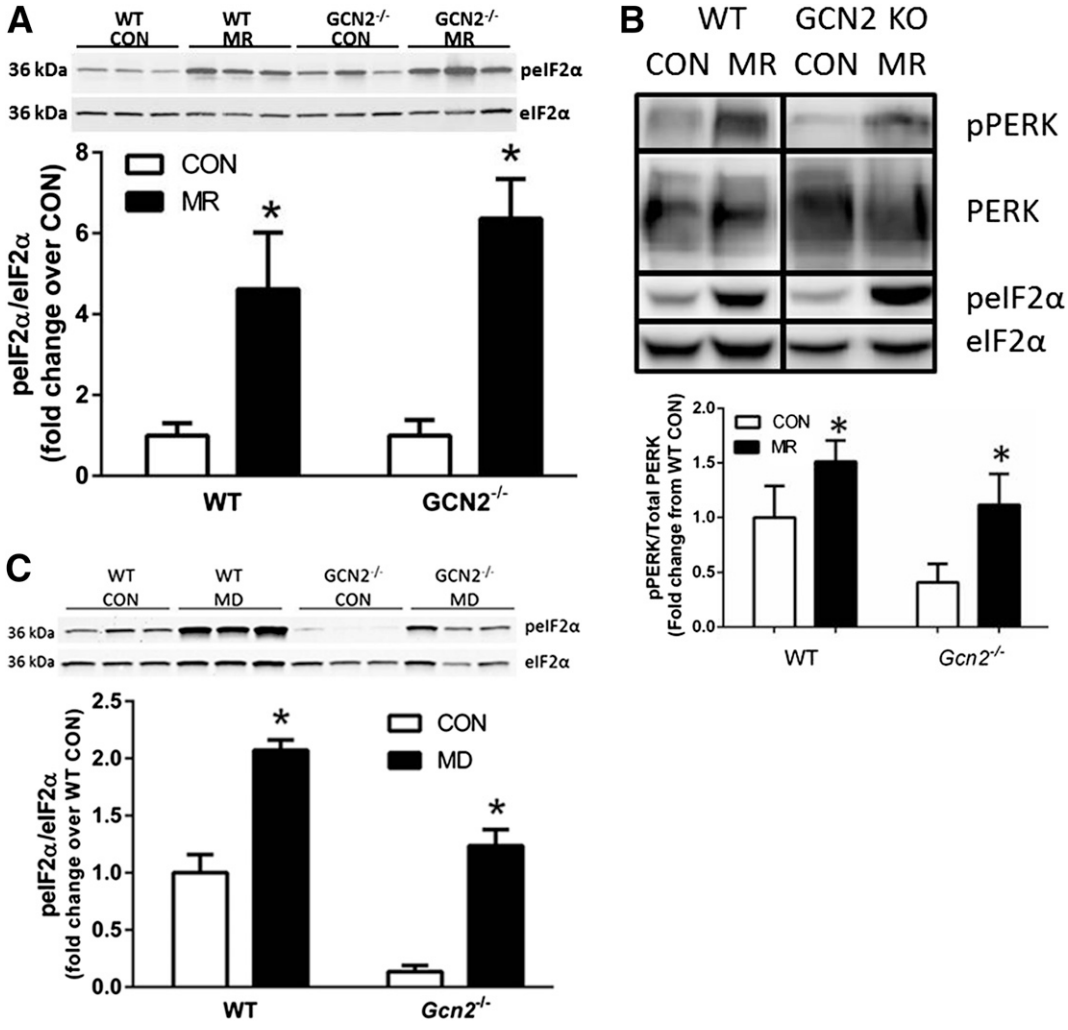

Figure 4—Effects of dietary MR on phosphorylation of hepatic eIF2α and PERK in *GCN2*$^{-/-}$ mice. *A*: The effect of the MR diet on eIF2α phosphorylation (peIF2α) in livers of WT and *Gcn2*$^{-/-}$ mice after 14 weeks of dietary MR. *B*: The effect of the MR diet on PERK phosphorylation (pPERK) in livers of WT and *Gcn2*$^{-/-}$ mice after 14 weeks of dietary MR. Fold changes in MR-induced eIF2α and PERK phosphorylation are expressed relative to the responses in mice of each genotype fed the CON diet. *C*: eIF2α phosphorylation in livers of WT and *Gcn*$^{-/-}$ mice after consuming CON or a diet devoid of methionine (0% methionine) for 6 days. Fold changes in methionine deprivation (MD)–induced eIF2α phosphorylation are expressed relative to WT mice fed the CON diet. Data are presented as mean ± SEM (n = 6–9). *Differ from CON within genotype at $P < 0.05$. KO, knockout.

GCN2 is not required for eIF2 phosphorylation by MR. Low-protein diets also increased eIF2 phosphorylation in *Gcn2*$^{-/-}$ mice (26), suggesting the presence of an alternative eIF2 kinase that is activated by MR and low-protein diets. One possibility is PERK, which is activated by ER stress and reductions in GSH (18,41). PERK phosphorylation was similarly increased by MR in WT and *Gcn2*$^{-/-}$ mice (Fig. 4*B*). To explore the involvement of PERK activation by MR, we tested the possibility that MR was disruptive to ER homeostasis and protein folding, eliciting an ER stress or UPR. Measurement of genetic markers that correspond with activation of the UPR showed that MR did not provoke ER stress in the livers of WT or *Gcn2*$^{-/-}$ mice (Table 2). To further explore the transcriptional consequences of PERK activation, we measured MR-dependent changes in known targets of ATF4 and the transcription factor NRF2, which is activated after phosphorylation by PERK (42). MR strongly induced the expression of eIF2/ATF4 genes, *Asns, Trib3, Gadd34,* and *Vldlr*, in livers of WT and *Gcn2*$^{-/-}$ mice (Table 2). Known targets of NRF2 were upregulated (*Aox1, Cbr1, Ephx1, Gsta1, Mgst3, Nqo1, Psat1,* and *Cyp4a14)* and downregulated (*Thrsp*), providing strong evidence that NRF2 was also activated by MR (Table 2). Together, these findings show that MR activates the ISR and NRF2 pathways regardless of GCN2 status and without induction of the UPR.

Experiment 4

Given the role of GCN2 in responding to LD (39) but not MR, we tested the possibility that GCN2 could distinguish between EAA deprivation and EAA restriction by measuring eIF2 phosphorylation in WT and *Gcn2*$^{-/-}$ mice after methionine deprivation. Methionine deprivation for 6 days increased eIF2 phosphorylation in livers of WT and *Gcn2*$^{-/-}$ mice, indicating that unlike LD, GCN2 is not required for the methionine deprivation–induced phosphorylation of eIF2 (Fig. 4*C*). Together, these studies illustrate that GCN2 does not direct either the short-term signaling responses to dietary MR or its long-term effects on energy balance or insulin sensitivity. The findings also

Table 2—Genetic markers of ER stress response, NRF2 transcriptional program, and integrated stress response (eIF2α/ATF4) in livers of WT and *Gcn2*$^{-/-}$ mice fed CON or MR diet for 14 weeks

		WT		*Gcn2*$^{-/-}$	
Gene symbol	Signaling pathway	CON	MR	CON	MR
Hspa5	ER stress	0.45 ± 0.06^{a}	0.46 ± 0.05^{a}	0.50 ± 0.07^{a}	0.37 ± 0.04^{a}
Ddit3	ER stress	0.49 ± 0.05^{a}	0.73 ± 0.16^{a}	0.42 ± 0.03^{a}	0.43 ± 0.02^{a}
Edem1	ER stress	0.45 ± 0.02^{a}	0.36 ± 0.02^{b}	0.37 ± 0.03^{b}	0.13 ± 0.01^{b}
Hsp90b1	ER stress	0.15 ± 0.02^{a}	0.14 ± 0.01^{a}	0.14 ± 0.02^{a}	0.11 ± 0.01^{a}
Herp	ER stress	0.24 ± 0.03^{a}	0.23 ± 0.02^{a}	0.24 ± 0.02^{a}	0.26 ± 0.01^{a}
Ibtk	ER stress	0.16 ± 0.01^{a}	0.15 ± 0.02^{a}	0.07 ± 0.01^{b}	0.08 ± 0.00^{b}
Txnip	ER stress	0.41 ± 0.04^{a}	0.51 ± 0.06^{a}	0.32 ± 0.04^{a}	0.33 ± 0.03^{a}
Aox1	NRF2	0.77 ± 0.07^{a}	1.35 ± 0.15^{b}	0.40 ± 0.06^{c}	0.99 ± 0.07^{b}
Cbr1	NRF2	0.32 ± 0.04^{a}	1.09 ± 0.25^{b}	0.33 ± 0.06^{a}	0.91 ± 0.18^{b}
Gsr	NRF2	0.31 ± 0.01^{a}	0.40 ± 0.02^{b}	0.27 ± 0.02^{a}	0.33 ± 0.02^{a}
Cyp4a14	NRF2	0.19 ± 0.04^{a}	0.59 ± 0.14^{b}	0.15 ± 0.06^{a}	0.23 ± 0.06^{a}
Ephx1	NRF2	0.26 ± 0.04^{a}	0.54 ± 0.06^{b}	0.25 ± 0.03^{a}	0.45 ± 0.08^{b}
Gsta2	NRF2	0.32 ± 0.05^{a}	2.85 ± 0.21^{b}	0.36 ± 0.07^{a}	2.54 ± 0.40^{b}
Mgst3	NRF2	0.13 ± 0.02^{a}	0.22 ± 0.02^{b}	0.12 ± 0.01^{a}	0.23 ± 0.03^{b}
Nqo1	NRF2	0.63 ± 0.10^{a}	1.35 ± 0.12^{b}	0.41 ± 0.07^{a}	0.85 ± 0.10^{b}
Psat1	NRF2	0.22 ± 0.04^{a}	2.35 ± 0.37^{b}	0.38 ± 0.16^{a}	2.27 ± 0.30^{b}
Txnrd1	NRF2	0.64 ± 0.03^{a}	0.98 ± 0.09^{b}	0.53 ± 0.04^{a}	0.70 ± 0.04^{c}
Thrsp	NRF2	0.53 ± 0.10^{a}	0.16 ± 0.03^{b}	0.73 ± 0.13^{a}	0.20 ± 0.04^{b}
Asns	ISR/eIF2/ATF4	0.32 ± 0.07^{a}	3.59 ± 0.32^{b}	0.23 ± 0.05^{a}	4.27 ± 0.38^{b}
Trib3	ISR/eIF2/ATF4	0.55 ± 0.02^{a}	1.05 ± 0.11^{b}	0.30 ± 0.02^{c}	0.94 ± 0.05^{b}
Vldlr	ISR/eIF2/ATF4	0.23 ± 0.06^{a}	1.32 ± 0.17^{b}	0.68 ± 0.10^{c}	2.02 ± 0.27^{d}
Gadd34	ISR/eIF2/ATF4	0.30 ± 0.03^{a}	0.45 ± 0.03^{b}	0.18 ± 0.03^{c}	0.31 ± 0.01^{a}

mRNA expression of markers of ER stress (*Hspa5*, *Ddit3*, *Edem1*, *Hsp90b1*, *Herp*, *Ibtk*, and *Txnip*), NRF2 transcriptional program (*Aox1*, *Cbr1*, *Gsr*, *Cyp4a14*, *Ephx1*, *Gsta1*, *Mgst3*, *Nqo1*, *Psat1*, *Txnrd1*, and *Thrsp*), and ISR/eIF2α/ATF4-regulated genes (*Asns*, *Trib3*, *Vldlr*, and *Gadd34*) in livers of WT and *Gcn2*$^{-/-}$ mice was determined by RT-PCR, expressed relative to cyclophilin, adjusted to comparable significant digits, and compared by two-way ANOVA to test for effects of genotype, diet, and genotype × diet interaction. Residual variance was used as the error term for post hoc testing of genotype × diet means for each gene using the Bonferroni correction. Within each gene, means annotated with different letters differ at $P < 0.05$.

show that PERK is sensitive to MR and activates the ISR but not the UPR in response to the diet.

Dietary Cysteine Reverses the Effects of MR

Experiments 5 and 6

To explore whether PERK activation was related to hepatic GSH, 0.2% cysteine was added back to the MR diet. This dietary addition reversed the reduction in hepatic GSH and the increase in nighttime EE by MR (Fig. 5*A*). The addition of cysteine also reversed the MR-induced increase in serum FGF21 and the reduction in fasting insulin (Fig. 5*B*). In addition, cysteine blocked the MR-induced increases in NRF2-sensitive and eIF2/ATF4-sensitive genes in the liver (Fig. 5*C*). To test whether adding back cysteine also reversed the activation of eIF2α and PERK, we measured the phosphorylation of hepatic eIF2α and PERK after 8 weeks of 0.12% MR or 0.12% MR plus 0.2% cysteine. Figure 6*A* illustrates that adding cysteine back reversed the MR-dependent activation of both eIF2α and PERK (Fig. 6*A*). These findings link the MR-induced reduction of GSH to activation of the ISR and significant components of the metabolic profile produced by the diet. A proposed model showing the GCN2-independent, GSH-dependent signaling through PERK to eIF2/ATF4 and NRF2 is shown in Fig. 6*B*.

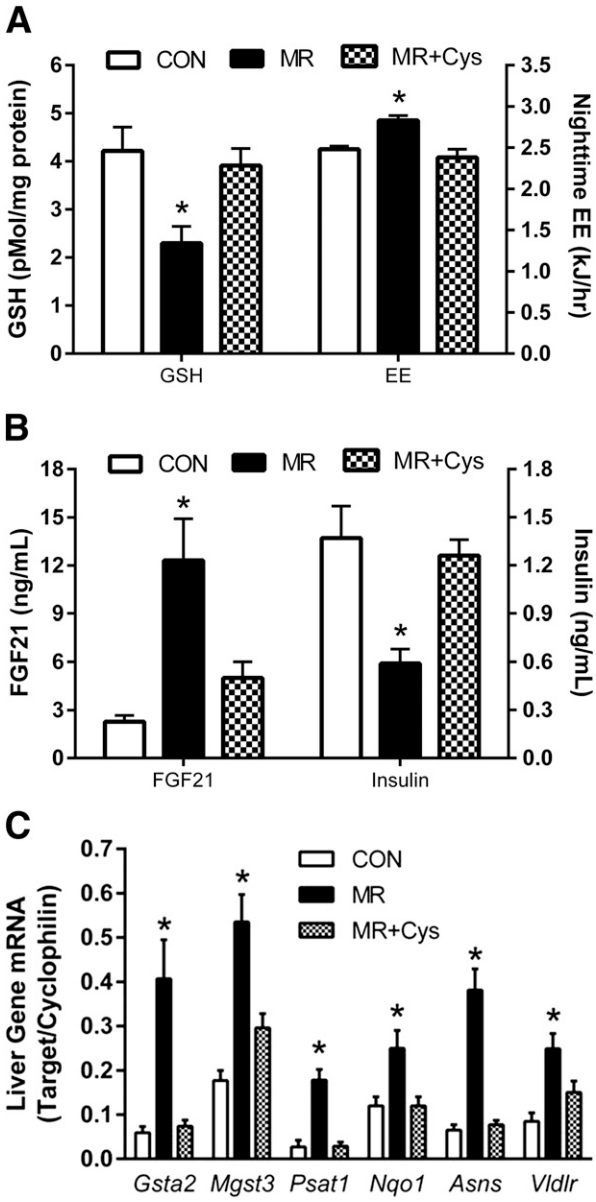

Figure 5—Effects of addition of cysteine (Cys) to effects of dietary MR on hepatic GSH, EE, FGF21, and insulin and hepatic gene expression. The responses of mice to an MR diet containing 0.2% cysteine were compared with the MR diet alone as described in RESEARCH DESIGN AND METHODS. *A*: The effects of cysteine on MR-dependent effects on hepatic GSH and nighttime EE. *B*: The effects of cysteine on MR-dependent effects on serum FGF21 and fasting insulin. *C*: The effect of cysteine on MR-dependent effects on NRF2-sensitive (*Gsta2*, *Mgst3*, *Psat1*, and *Nqo1*) and eIF2α/ATF4-sensitive (*Asns* and *Vldlr*) genes in the liver. Data are presented as mean ± SEM (n = 8). *Differ from corresponding CON at $P < 0.05$. hr, hour.

DISCUSSION

The original report of dietary MR showed that ad libitum consumption of a diet containing 0.17% methionine and no cysteine increased longevity in rats by 25–30% (43,44). The paradoxical finding that MR also reduced adiposity despite increasing food intake focused growing interest on the short-term metabolic effects of this diet. The responses include increased food intake, increased EE, reduced fat deposition, increased insulin sensitivity, reduced tissue and circulating lipids, and tissue-specific transcriptional effects (1–6,45,46). In the present work, a loss-of-function approach was used to test whether GCN2 is an essential mediator of these metabolic responses to MR. Using a combination of metabolic phenotyping and examination of tissue-specific responses, we provide compelling evidence that GCN2 is not required for the metabolic and adaptive responses to dietary MR. In contrast, we provide evidence that MR signals to eIF2/ATF4 and NRF2 through the eIF2 kinase, PERK, which is activated by MR in the absence of ER stress. The result is activation of both the ISR, through eIF2/ATF4, and the NRF2-sensitive antioxidant response program (Table 2). Based on the significance of reduced formation of hepatic GSH to enhancement of insulin signaling in MR mice and HepG2 cells (27), we hypothesize that the reduced formation of hepatic GSH also represents a key metabolite through which dietary MR is affecting signaling through a novel PERK-eIF2-ATF4-NRF2 pathway.

Significant progress has been made in identifying molecular and cellular mechanisms of EAA sensing (30,39,47–53), but the more difficult challenge has been to understand how these sensing systems are anatomically and temporally organized to produce the complex physiological responses that occur when an EAA reduction is detected. Restricting the availability of EAAs activates GCN2, and previous studies have shown that GCN2 is an important mediator of some but not all of the effects of a diet lacking leucine (15,16). Stated another way, these findings illustrate

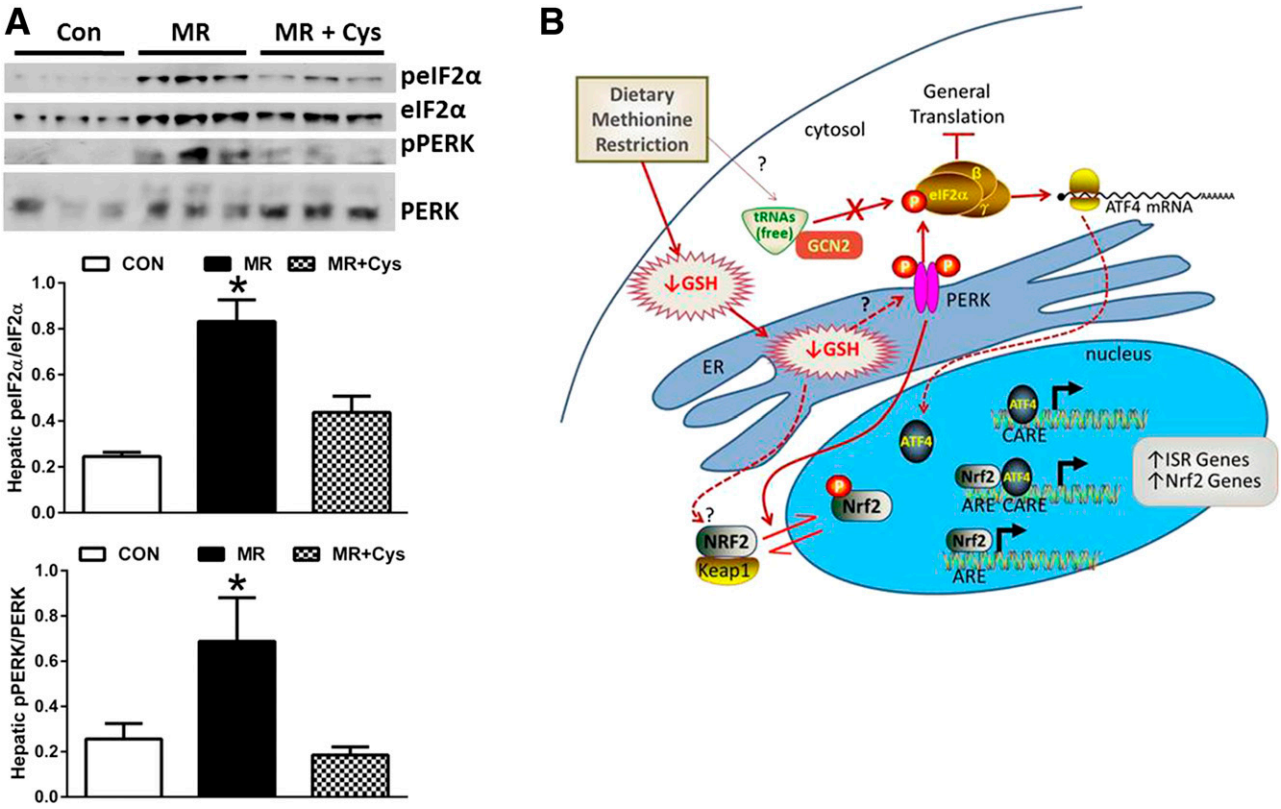

Figure 6—Effects of addition of cysteine (Cys) to effects of dietary MR on hepatic eIF2α and PERK phosphorylation. The effect of a 0.12% MR diet containing 0.2% cysteine was compared with the 0.12% MR diet alone as described in RESEARCH DESIGN AND METHODS. *A*: Band densities of phosphorylated eIF2α (peIF2α) and phosphorylated PERK (pPERK) were expressed relative to total eIF2α and PERK, respectively, and compared by ANOVA. Data are presented as mean ± SEM (n = 8). *Differ from the CON group at $P < 0.05$. *B*: Schematic model of proposed mechanisms of GCN2-independent signaling by dietary MR in the liver. The diet-induced decrease is GSH activates PERK, which is proposed to activate eIF2/ATF4, NRF2, and their corresponding ISR and NRF2 transcriptional programs. ARE, antioxidant response element; CARE, C/EBP ATF response element.

that mechanisms additional to GCN2 sense and respond to the absence of leucine. The role of GCN2 as a mediator of EAA restriction, particularly restriction of methionine, is unknown. There is an assumption that any degree of EAA restriction sufficient to activate GCN2 would produce a common set of responses, but clear exceptions are evident with leucine. For example, LD (e.g., 100% restriction) causes a significant decrease in food intake and lipogenic gene expression in the liver (15), whereas leucine restriction by 85% increases food consumption and has no effect on hepatic lipogenic genes (54). It is unclear whether GCN2 is comparably activated by these two diets, but the responses to them are fundamentally different. While the present work widens the apparent conundrum by showing that MR is fully effective without GCN2, these results are consistent with an array of recent reports defining unique molecular events after the removal of different amino acids from cells in culture (55–57). Together, these findings emphasize that both the EAA being restricted and the degree of restriction play important roles in determining the responses to EAA-modified diets.

The uniqueness of methionine was illustrated in previous work showing that the decrease in hepatic GSH produced by MR extends the activation cycle of insulin signaling to protein kinase B by slowing the dephosphorylation of phosphatidylinositol (3,4,5)-triphosphate (27). This occurs because reducing dietary methionine limits the formation of the GSH precursor, cysteine, and the resulting reduction of GSH limits GSH-dependent degradation of phosphatidylinositol (3,4,5)-triphosphate by phosphatase and tensin homolog (27). The present work extends these findings by proposing that MR increases ATF4-sensitive genes by activating PERK. Surprisingly, markers of ER stress, the normal activator of PERK, were unchanged, indicating that MR was not activating PERK as part of the UPR. Given the essential role of GSH in disulfide bond formation during protein folding in the ER (18,58), it seems plausible that the MR-dependent decrease in hepatic GSH, rather than an accumulation of misfolded proteins, is an alternate signal for PERK activation (19). For example, although PERK is activated by glucose restriction in ESCs, its activation depends on depletion of cellular GSH (41). PERK is not typically activated by EAA depletion (41), so it seems likely that the ability of MR to activate PERK and initiate components of the ISR derives from its unique effects on hepatic GSH. In

addition to eIF2, our findings indicate that the NRF2-dependent antioxidant response program is activated by MR. NRF2 is activated by PERK (42), although NRF2 transcriptional activity also responds to low GSH (59). It is interesting that the ISR and the antioxidant stress response share genes whose primary function is to increase production of GSH (19). Our findings suggest the interesting possibility that PERK activation by low GSH may be the common signal.

The ability of MR to produce its full range of metabolic effects is not compromised in *Gcn2*$^{-/-}$ mice, and we have proposed that hepatic PERK, activated by the decrease in hepatic GSH, is a critical sensing event linking the MR diet to its effects. We have supported this hypothesis by showing that within hours, dietary MR activates hepatic *Fgf21* and increases its circulating levels. Based on the known physiological effects of FGF21 (34,36,60,61), the MR-induced browning of WAT, activation of thermogenesis in BAT, increase in EE, and overall increase in insulin sensitivity are fully consistent with the MR-induced increase in hepatic FGF21 (27,62). In addition, we show that the MR-dependent increase in EE and UCP1 expression in IWAT is dependent on FGF21. We have also shown that FGF21 acts directly in adipose tissue to enhance basal and insulin-dependent glucose uptake (27). Third, we have shown that the MR-dependent decrease in hepatic GSH amplifies insulin-dependent signaling in the liver (27). The central importance of reduced GSH to the metabolic phenotype is illustrated through a gain-of-function approach produced by adding back a small amount of the GSH precursor, cysteine (0.2%), to the MR diet. If cysteine repletion restored hepatic GSH levels and hepatic GSH was critical to *Fgf21* transactivation, we predicted that FGF21 and other components of the phenotype would be reversed. This is precisely what was observed. The addition of cysteine to the MR diet restored hepatic GSH to control levels, along with plasma FGF21, EE, NRF2- and ATF4-sensitive genes, fasting insulin, and eIF2α phosphorylation. Collectively, our findings provide the first evidence of a nutrient-sensing system for MR that bypasses GCN2 and activates hepatic PERK through a noncanonical GSH-dependent mechanism.

Acknowledgments. The authors thank Cindi Tramonte for administrative support and Manda Orgeron, Alicia Pierse, Alexandra N. Daniel, and Phillip H. Behrens for excellent technical support. Cindi Tramonte, Manda Orgeron, and Alicia Pierce are at the Pennington Biomedical Research Center (Baton Rouge, LA), and Alexandra N. Daniel and Phillip H. Behrens are in Biochemistry and Molecular Biology, Indiana University School of Medicine-Evansville, Evansville, IN. The authors thank Carrie Elks at Pennington Biomedical Research Center (Baton Rouge, LA) for her valuable input on Western blotting of PERK.

Duality of Interest. No potential conflicts of interest relevant to this article were reported.

Author Contributions. D.W., T.G.A., and T.W.G. contributed to the writing and editing of the manuscript. D.W., K.P.S., L.A.F., C.C.C., K.N.D., and J.S. conducted the animal experiments. D.W., K.P.S., L.A.F., K.N.D., J.S., M.X., E.C.H., I.A.N., and A.P.P. conducted the in vitro analysis and associated Western blots and mRNA and metabolite measurements. T.G.A. and T.W.G. analyzed data used to produce illustrations. T.W.G. is the guarantor of this work and, as such, had full access to all the data in the study and takes responsibility for the integrity of the data and the accuracy of the data analysis.

Funding. This work was supported in part by the American Diabetes Association (1-12-BS-58 to T.W.G.), National Institutes of Health (NIH) (RO1-HD-070487 to T.G.A. and RO1-DK-096311 to T.W.G.), U.S. Department of Agriculture Cooperative State Research, Education, and Extension Service (Multistate NC1184 to T.G.A.), and the Vanderbilt University Mouse Metabolic Phenotyping Center (NIH U24-DK-059637). This work also made use of the Genomics core facilities supported by NIH P20-GM-103528 to T.W.G. and NIH 2P30-DK-072476. D.W. was supported by NIH National Research Service Award 1 F32-DK-098918 and NIH P20-GM-103528. L.A.F. is supported by an ADA mentor-based postdoctoral fellowship (7-13-MI-05). E.C.H. was supported by summer student fellowship (NIH 5T35OD011151). A.P.P. is supported by an NIH Institutional Research and Academic Career Development Award (New Jersey/New York for Science Partnerships in Research & Education at Rutgers-Robert Woods Johnson Medical School).

References

1. Malloy VL, Krajcik RA, Bailey SJ, Hristopoulos G, Plummer JD, Orentreich N. Methionine restriction decreases visceral fat mass and preserves insulin action in aging male Fischer 344 rats independent of energy restriction. Aging Cell 2006; 5:305–314

2. Hasek BE, Stewart LK, Henagan TM, et al. Dietary methionine restriction enhances metabolic flexibility and increases uncoupled respiration in both fed and fasted states. Am J Physiol Regul Integr Comp Physiol 2010;299:R728–R739

3. Plaisance EP, Henagan TM, Echlin H, et al. Role of β-adrenergic receptors in the hyperphagic and hypermetabolic responses to dietary methionine restriction. Am J Physiol Regul Integr Comp Physiol 2010;299:R740–R750

4. Hasek BE, Boudreau A, Shin J, et al. Remodeling the integration of lipid metabolism between liver and adipose tissue by dietary methionine restriction in rats. Diabetes 2013;62:3362–3372

5. Perrone CE, Mattocks DA, Jarvis-Morar M, Plummer JD, Orentreich N. Methionine restriction effects on mitochondrial biogenesis and aerobic capacity in white adipose tissue, liver, and skeletal muscle of F344 rats. Metabolism 2010; 59:1000–1011

6. Perrone CE, Mattocks DA, Hristopoulos G, Plummer JD, Krajcik RA, Orentreich N. Methionine restriction effects on 11 -HSD1 activity and lipogenic/lipolytic balance in F344 rat adipose tissue. J Lipid Res 2008;49:12–23

7. Sood R, Porter AC, Olsen DA, Cavener DR, Wek RC. A mammalian homologue of GCN2 protein kinase important for translational control by phosphorylation of eukaryotic initiation factor-2alpha. Genetics 2000;154:787–801

8. Visweswaraiah J, Lageix S, Castilho BA, et al. Evidence that eukaryotic translation elongation factor 1A (eEF1A) binds the Gcn2 protein C terminus and inhibits Gcn2 activity. J Biol Chem 2011;286:36568–36579

9. Seo J, Fortuno ES 3rd, Suh JM, et al. Atf4 regulates obesity, glucose homeostasis, and energy expenditure. Diabetes 2009;58:2565–2573

10. Yoshizawa T, Hinoi E, Jung DY, et al. The transcription factor ATF4 regulates glucose metabolism in mice through its expression in osteoblasts. J Clin Invest 2009;119:2807–2817

11. De Sousa-Coelho AL, Marrero PF, Haro D. Activating transcription factor 4-dependent induction of FGF21 during amino acid deprivation. Biochem J 2012; 443:165–171

12. Kilberg MS, Shan J, Su N. ATF4-dependent transcription mediates signaling of amino acid limitation. Trends Endocrinol Metab 2009;20:436–443

13. Hao S, Sharp JW, Ross-Inta CM, et al. Uncharged tRNA and sensing of amino acid deficiency in mammalian piriform cortex. Science 2005;307:1776–1778

14. Anthony TG, Gietzen DW. Detection of amino acid deprivation in the central nervous system. Curr Opin Clin Nutr Metab Care 2013;16:96–101

15. Guo F, Cavener DR. The GCN2 eIF2alpha kinase regulates fatty-acid homeostasis in the liver during deprivation of an essential amino acid. Cell Metab 2007; 5:103–114

16. Anthony TG, McDaniel BJ, Byerley RL, et al. Preservation of liver protein synthesis during dietary leucine deprivation occurs at the expense of skeletal muscle mass in mice deleted for eIF2 kinase GCN2. J Biol Chem 2004;279:36553–36561
17. Anthony TG, Morrison CD, Gettys TW. Remodeling of lipid metabolism by dietary restriction of essential amino acids. Diabetes 2013;62:2635–2644
18. Harding HP, Zhang Y, Zeng H, et al. An integrated stress response regulates amino acid metabolism and resistance to oxidative stress. Mol Cell 2003;11:619–633
19. Donnelly N, Gorman AM, Gupta S, Samali A. The eIF2α kinases: their structures and functions. Cell Mol Life Sci 2013;70:3493–3511
20. Dang Do AN, Kimball SR, Cavener DR, Jefferson LS. eIF2alpha kinases GCN2 and PERK modulate transcription and translation of distinct sets of mRNAs in mouse liver. Physiol Genomics 2009;38:328–341
21. Wek RC, Jiang HY, Anthony TG. Coping with stress: eIF2 kinases and translational control. Biochem Soc Trans 2006;34:7–11
22. Shin S, Buel GR, Wolgamott L, et al. ERK2 mediates metabolic stress response to regulate cell fate. Mol Cell 2015;59:382–398
23. Hamanaka RB, Bennett BS, Cullinan SB, Diehl JA. PERK and GCN2 contribute to eIF2alpha phosphorylation and cell cycle arrest after activation of the unfolded protein response pathway. Mol Biol Cell 2005;16:5493–5501
24. Liu Y, László C, Liu Y, et al. Regulation of G(1) arrest and apoptosis in hypoxia by PERK and GCN2-mediated eIF2alpha phosphorylation. Neoplasia 2010;12:61–68
25. Lee J, Ozcan U. Unfolded protein response signaling and metabolic diseases. J Biol Chem 2014;289:1203–1211
26. Laeger T, Henagan TM, Albarado DC, et al. FGF21 is an endocrine signal of protein restriction. J Clin Invest 2014;124:3913–3922
27. Stone KP, Wanders D, Orgeron M, Cortez CC, Gettys TW. Mechanisms of increased in vivo insulin sensitivity by dietary methionine restriction in mice. Diabetes 2014;63:3721–3733
28. Ayala JE, Bracy DP, McGuinness OP, Wasserman DH. Considerations in the design of hyperinsulinemic-euglycemic clamps in the conscious mouse. Diabetes 2006;55:390–397
29. Gietzen DW, Hao S, Anthony TG. Mechanisms of food intake repression in indispensable amino acid deficiency. Annu Rev Nutr 2007;27:63–78
30. Gietzen DW, Ross CM, Hao S, Sharp JW. Phosphorylation of eIF2alpha is involved in the signaling of indispensable amino acid deficiency in the anterior piriform cortex of the brain in rats. J Nutr 2004;134:717–723
31. Wu J, Cohen P, Spiegelman BM. Adaptive thermogenesis in adipocytes: is beige the new brown? Genes Dev 2013;27:234–250
32. Wanders D, Burk DH, Cortez CC, et al. UCP1 is an essential mediator of the effects of methionine restriction on energy balance but not insulin sensitivity. FASEB J 2015;29:2603–2615
33. Wilson GJ, Lennox BA, She P, et al. GCN2 is required to increase fibroblast growth factor 21 and maintain hepatic triglyceride homeostasis during asparaginase treatment. Am J Physiol Endocrinol Metab 2015;308:E283–E293
34. Coskun T, Bina HA, Schneider MA, et al. Fibroblast growth factor 21 corrects obesity in mice. Endocrinology 2008;149:6018–6027
35. Sarruf DA, Thaler JP, Morton GJ, et al. Fibroblast growth factor 21 action in the brain increases energy expenditure and insulin sensitivity in obese rats. Diabetes 2010;59:1817–1824
36. Owen BM, Ding X, Morgan DA, et al. FGF21 acts centrally to induce sympathetic nerve activity, energy expenditure, and weight loss. Cell Metab 2014;20:670–677
37. Xiao F, Yu J, Guo Y, et al. Effects of individual branched-chain amino acids deprivation on insulin sensitivity and glucose metabolism in mice. Metabolism 2014;63:841–850
38. Xiao F, Huang Z, Li H, et al. Leucine deprivation increases hepatic insulin sensitivity via GCN2/mTOR/S6K1 and AMPK pathways. Diabetes 2011;60:746–756
39. Zhang P, McGrath BC, Reinert J, et al. The GCN2 eIF2alpha kinase is required for adaptation to amino acid deprivation in mice. Mol Cell Biol 2002;22:6681–6688
40. Bunpo P, Dudley A, Cundiff JK, Cavener DR, Wek RC, Anthony TG. GCN2 protein kinase is required to activate amino acid deprivation responses in mice treated with the anti-cancer agent L-asparaginase. J Biol Chem 2009;284:32742–32749
41. Cullinan SB, Diehl JA. PERK-dependent activation of Nrf2 contributes to redox homeostasis and cell survival following endoplasmic reticulum stress. J Biol Chem 2004;279:20108–20117
42. Cullinan SB, Zhang D, Hannink M, Arvisais E, Kaufman RJ, Diehl JA. Nrf2 is a direct PERK substrate and effector of PERK-dependent cell survival. Mol Cell Biol 2003;23:7198–7209
43. Orentreich N, Matias JR, DeFelice A, Zimmerman JA. Low methionine ingestion by rats extends life span. J Nutr 1993;123:269–274
44. Richie JP Jr, Leutzinger Y, Parthasarathy S, Malloy V, Orentreich N, Zimmerman JA. Methionine restriction increases blood glutathione and longevity in F344 rats. FASEB J 1994;8:1302–1307
45. Sun L, Sadighi Akha AA, Miller RA, Harper JM. Life-span extension in mice by preweaning food restriction and by methionine restriction in middle age. J Gerontol A Biol Sci Med Sci 2009;64:711–722
46. Johnson JE, Johnson FB. Methionine restriction activates the retrograde response and confers both stress tolerance and lifespan extension to yeast, mouse and human cells. PLoS One 2014;9:e97729
47. Kimball SR. Regulation of global and specific mRNA translation by amino acids. J Nutr 2002;132:883–886
48. Kobayashi H, Børsheim E, Anthony TG, et al. Reduced amino acid availability inhibits muscle protein synthesis and decreases activity of initiation factor eIF2B. Am J Physiol Endocrinol Metab 2003;284:E488–E498
49. Pham PTT, Heydrick SJ, Fox HL, Kimball SR, Jefferson LS Jr, Lynch CJ. Assessment of cell-signaling pathways in the regulation of mammalian target of rapamycin (mTOR) by amino acids in rat adipocytes. J Cell Biochem 2000;79:427–441
50. Gietzen DW. Neural mechanisms in the responses to amino acid deficiency. J Nutr 1993;123:610–625
51. Deval C, Chaveroux C, Maurin AC, et al. Amino acid limitation regulates the expression of genes involved in several specific biological processes through GCN2-dependent and GCN2-independent pathways. FEBS J 2009;276:707–718
52. Siu F, Bain PJ, LeBlanc-Chaffin R, Chen H, Kilberg MS. ATF4 is a mediator of the nutrient-sensing response pathway that activates the human asparagine synthetase gene. J Biol Chem 2002;277:24120–24127
53. Pan Y, Chen H, Siu F, Kilberg MS. Amino acid deprivation and endoplasmic reticulum stress induce expression of multiple activating transcription factor-3 mRNA species that, when overexpressed in HepG2 cells, modulate transcription by the human asparagine synthetase promoter. J Biol Chem 2003;278:38402–38412
54. Wanders D, Stone KP, Dille K, Simon J, Pierse A, Gettys TW. Metabolic responses to dietary leucine restriction involve remodeling of adipose tissue and enhanced hepatic insulin signaling. Biofactors 2015;41:391–402
55. Wolfson RL, Chantranupong L, Saxton RA, et al. Sestrin2 is a leucine sensor for the mTORC1 pathway. Science 2016;351:43–48
56. Tang X, Keenan MM, Wu J, et al. Comprehensive profiling of amino acid response uncovers unique methionine-deprived response dependent on intact creatine biosynthesis. PLoS Genet 2015;11:e1005158
57. Wang S, Tsun ZY, Wolfson RL, et al. Metabolism. Lysosomal amino acid transporter SLC38A9 signals arginine sufficiency to mTORC1. Science 2015;347:188–194
58. Harding HP, Zhang Y, Ron D. Protein translation and folding are coupled by an endoplasmic-reticulum-resident kinase. Nature 1999;397:271–274
59. Nguyen T, Nioi P, Pickett CB. The Nrf2-antioxidant response element signaling pathway and its activation by oxidative stress. J Biol Chem 2009;284:13291–13295
60. Douris N, Stevanovic DM, Fisher FM, et al. Central fibroblast growth factor 21 browns white fat via sympathetic action in male mice. Endocrinology 2015;156:2470–2481
61. Kharitonenkov A, Shiyanova TL, Koester A, et al. FGF-21 as a novel metabolic regulator. J Clin Invest 2005;115:1627–1635
62. Patil YN, Dille KN, Burk DH, Cortez CC, Gettys TW. Cellular and molecular remodeling of inguinal adipose tissue mitochondria by dietary methionine restriction. J Nutr Biochem 2015;26:1235–1247